Functioning of the multilinear lag-cascade flood routing model as a means of transporting pollutants in the river

Jafar Chabokpour, Barkha Chaplot, Mehdi Dasineh, Amir Ghaderi and Hazi Md Azamathulla

ABSTRACT

The purpose of this paper is to use the application of the multilinear lag cascade model as a contaminant transport model through river networks. Monocacy River and Antietam Creek data, which were collected by USGS with different reach lengths and discharge conditions, have been used in the current study. It was found that the multilinear discrete lag-cascade (MDLC) model is capable of reconstructing contaminant breakthrough curves. A complete study was performed to estimate the reach length for use in the accurate simulation, and it was concluded that by assuming a uniform flow through the reach, the length unit should be obtained by applying Pe = 12. Moreover, by using temporal moment matching, explicit relationships for MDLC model parameters (k, n, and τ) and based on conventional advection-dispersion equation (ADE) parameters (D, u, x) were extracted. MDLC parameters of the field breakthrough curves were extracted, and it was found that the increase of Pe number caused an increase in delay time and the number of cascades. However, the residence time was obtained to be fixed. Additionally, by assuming the dispersivity parameter (D/u) is constant, the changes in the MDLC parameters were investigated by velocity variation, and new relationships were proposed to estimate the parameters under different hydraulic conditions. Using presented equations provided in this study for residence time (k), cascade number (n), and delay time (τ), the sensitivity analysis was performed, and it was found that the parameters of velocity (u), dispersion coefficient (D), and velocity (u) have the most important effect in calculation of them, respectively.

Key words | contaminant transport, MDLC model, multi-linear cascades, river reach

Jafar Chabokpour (corresponding author)
Civil Engineering Department,
University of Maragheh,
Maragheh,
Iran
E-mail: *j.chabokpour@maragheh.ac.ir*

Barkha Chaplot
Department of Geography, MJK College,
BRA Bihar University,
Muzaffarpur,
India

Mehdi Dasineh
Civil Engineering Department,
University of Marageh,
Maragheh,
Iran

Amir Ghaderi
Department of Civil Engineering,
Faculty of Engineering,
University of Zanjan,
Zanjan,
Iran
and
Department of Civil Engineering,
University of Calabria,
87036 Arcavacata, Rende,
Italy

Hazi Md Azamathulla
Civil and Environmental Engineering,
University of the West Indies,
St. Augustine, Trinidad,
West Indies

HIGHLIGHTS

- The efficiency of the multilinear lag cascade model was demonstrated as a contaminant transport model.
- Relationships were derived for estimating the MDLC parameters by matching its temporal moments with the classical ADE model.
- Sensitivity analysis of residence time (k), cascade number (n), and delay time (τ) showed that the parameters of velocity (u), dispersion coefficient (D), and velocity (u) have the most significant impact on their estimation, respectively.
- It was observed that by changing the flow velocity in the river reach, it is possible to estimate the amount of new parameters from the previous parameters using the presented equations.

doi: 10.2166/ws.2020.181

INTRODUCTION

The use of simple methods in flood forecasting systems and construction of river reaches' flood control structures has been popular in the past few years. The general mathematical framework for simulating dynamic wave propagation, including continuity and momentum equations, is one-dimensional Saint-Venant equations. The complete solution has some difficulties and requires precision in the input data. Such complexities led to the development of simpler methods for rapid response in downstream rivers (Keefer & McQuivey 1974; Becker 1976; Kundzewicz 1984; Becker & Kundzewicz 1987; Perumal 1992, 1994). Field hydrologists stated earlier that stage-hydrograph flood routing is better and more effective than discharge hydrographs (Spada *et al.* 2017; Cimorelli *et al.* 2018). In addition, the investigators focused on using simple methods that could simulate the nonlinear features of flood propagation. One of the most common approaches to flood routing simulation is multi-linear methods, which inherently have the dynamic characteristics of flood spreading. Perumal (1994) proposed a discrete-cascade multi-linear model as a flood routing system and accepted its implementation. Later Camacho & Lees (1999), by adding a time-delay parameter to the basic model, expanded the model and transformed it from a two-parameter simulation approach to a three-parameter one. A series of interconnected reservoirs with equivalent flood residence times were generated in the multi-linear methods, and the dynamic properties of the system were simulated through the operation of **n** number of them. Each input hydrograph was split into several ordinates with temporal discretization during the operation of this system. The discretization of the input hydrographs was often performed in the vertical direction, meaning that the time distribution scheme was applied (Bhabagrahi *et al.* 2019). It was noted that the scheme for time distribution is a safer way to interpret flood waves nonlinearly (Kundzewicz 1984; Becker & Kundzewicz 1987). The model parameters were changed in different time steps in the Multilinear Muskingum flood routing method. However, most of the simpler presented approaches used constant model parameters, and their function is based on many linear interconnected systems (Perumal 1992, 1994; Perumal & Sahoo 2007). In addition, many field hydrologists stated that depth-based routing methods with acceptable accuracies are more effective than discharge-based routing methods because of their simplicity of operation. A detailed and thorough explanation of the model is needed in order to understand it as a model for pollutant transport.

In water supply projects, accurate modeling of contaminant transport through the river reaches is important. Pollution transport has historically been computed using the one-dimensional advection-dispersion equation (ADE) by assuming absolute transverse mixing (Taylor 1953, 1954). Previous researches examined the operation of ADE model by conducting experimental and field tests (Elder 1959; Godfrey & Frederick 1963; Fischer 1966, 1967, 1968; Sayre & Chang 1968), and consequently it was observed that the acquired breakthrough curves (BC) are more skewed than the Taylor model can simulate. It was found that deviation from ADE simulation is the result of temporary trapping of the contaminant mass through dead zones of natural channels, which is also evident in the long tail of extracted BC curves. To solve the above problem, several types of models were previously presented for more accurate construction of the BC curves (Hays *et al.* 1966; Pedersen 1977; Haggerty *et al.* 2000; Boano *et al.* 2007; Marion *et al.* 2008). The mass exchange of contaminants between the main flow and dead zones was represented in all of the presented models using parameters such as residence time and transfer rate. In a number of previous studies, the impact of bed shapes and morphological processes such as bars and meanders on contaminant transport have also been studied (Jackson *et al.* 2013; Boano *et al.* 2014). Additionally, the effects of vegetation were also examined in the transport of pollutants due to changes in the velocity distribution and mixing coefficients (Shucksmith *et al.* 2010; Nepf 2012; Battiato & Rubol 2014; Musner *et al.* 2014; Rubol *et al.* 2016). The transient storage model (TS) was presented as a common storage model by combining first-order mass exchange between the main flow and storage area (Bencala & Walters 1983). The residence time of the pollutants in the storage zone was found to increase by the increases in the distance from the pollution source. Later, Bottacin-Busolin

et al. (2011) and Gooseff et al. (2013) proved that the TS model parameters are dependent upon the river reach length. A dual-zone version of the TS model firstly was presented by Choi et al. (2000) and then developed and operated by (Gooseff et al. 2004; Briggs et al. 2009; Bottacin-Busolin et al. 2011). Haggerty et al. (2000) presented the mathematical framework of multi-rate contaminant transport, and its applicability was proved using field data from the mountain stream, assuming power residence time distribution. Continuous time random walk model was used by Boano et al. (2007) to investigate the storage effect of contaminant transport through river reaches with the same assumption of power type distribution of the residence time parameter. This theory was then developed by Sherman et al. (2019) who presented a one-dimensional coupled time tandem walk, and proved its efficiency with synthetic numerical data. The effect of turbulence diffusion on the flow and bed boundaries has recently been investigated using numerical (Breugem et al. 2006; Sherman et al. 2019) and experimental (de Lemos 2005; Higashino et al. 2009; Azamathulla & Wu 2011; Azamathulla & Ahmad 2012; Chandler et al. 2016; Voermans et al. 2017; Roche et al. 2019; Chabokpour 2020) approaches. Fractional dispersion approaches in the pollution transport simulation through rivers have been extensively focused recently (Deng et al. 2006; Kelly et al. 2017).

By focusing on the mentioned literature, flood routing in the river reaches, it was found that it is also essential to investigate the contaminant transport through the river reaches by operation of more straightforward and accurate methods. Because of the similarity in the configuration of flood hydrographs and pollution breakthrough curves, the operation of a simple multilinear lag cascade model is reasonable. Therefore, the present study was designed to check the efficacy of the aforementioned method using the Monocacy and Antietam Creek field data. In addition to the above, the sensitivity of the model parameters was also investigated.

MATERIALS AND METHODS

Data collection

Field data from mass conservative tracer tests conducted by the US Geological Survey (USGS) at the Monocacy River and Antietam Creek were used to examine the performance of the MDLC model. Full details of the data collection condition by USGS were presented by Nordin & Sabol (1974). It is noteworthy that operated tracer in the tests was Rhodamine WT, which is a mass conservative contaminant. The details of the used data are listed in Table 1, in which the distance was measured from the pollutant injection site.

Model definition

During the multilinear model operation, the input stage hydrograph is divided into the vertical ordinates with fixed

Table 1 | Tracer injection data

River name and date of data collection	Site no.	Distance L (km)	Reach discharge Q (m^3/s)	Maximum observed concentration C max (ppb)	Time of maximum concentration t_p (hr)	Mean time of BC curve $\bar{t}$ (hr)	Variance of BC curve σ_t^2 (hr^2)	Skewness coefficient of BC curve
Monocacy River (June, 7, 1968)	1	6.4	14.32	18.5	7.1	7.91	1.11	1.58
	2	11.4	15.18	11.54	13.6	14.25	1.98	1.06
	3	16.65	15.89	9.17	19.6	20.36	2.64	0.72
	4	21.3	18.01	7.22	25.8	26.56	5.04	1.05
Antietam Creek (24, March, 1970)	1	1.6	5.1	331	1.35	1.45	0.044	1.80
	2	5.95	5.24	145.74	5.5	5.69	0.252	2
	3	13.33	7.37	76.41	15.9	16.23	1.582	3.07
	4	18.40	7.8	38.9	23.4	24.01	2.161	2
	5	26.25	8.51	36.93	33.2	34.02	4.323	1.62
	6	30.55	10.21	34.72	33	38.55	3.585	.01
	7	36.8	12.2	32.07	43.3	44.37	5.005	1.1
	8	41.45	12.76	28.04	47.4	48.20	6.002	1.15

time steps. Then, each pulse of entrance ordinates is routed using a separate sub-model. The final outflow can be achieved by summation of routed pulses. It has been mentioned earlier that Nash's discrete form of multilinear cascade model (Nash 1960) is superior in operation as opposed to the continuous time version (Bhabagrahi *et al.* 2019). Also, the multilinear lag cascade model (MDLC) was called a triple parameter version of the cascade model. It is one of the most widely used variants of multilinear models, which seem to be more suitable for simulating contaminant transport through the rivers. The schematic conceptual view of the MDLC model and its operation is depicted in Figure 1.

The impulse response function of a stage hydrograph with Δt discretization duration of MDLC approach is presented as Equations (1) and (2) (O'Connor 1976; Perumal 1994):

$$h_m = \left(\frac{\Delta t}{\Delta t + k_d}\right)^{n_d} \quad \text{for } m = 1 \tag{1}$$

$$h_m = \left(\frac{k_d}{\Delta t + k_d}\right)\left(\frac{m + n_d - 2}{m - 1}\right) h_{m-1} \quad \text{for } m > 1 \tag{2}$$

where: h_1 is the impulse response function associated with $t = \Delta t$, h_m is the impulse response function associated with $t = m\Delta t$, $m = 2 \ldots M$ and M is a sufficiently large number that h_m reduces to zero, Δt is time interval, and k_d, n_d are the discrete parameters of the Nash model, which are related to continuous time parameters according to Equations (3) and (4):

$$k_d = k - \Delta \tag{3}$$

$$n_d = \left(\frac{nk - \Delta t}{k - \Delta t}\right) \tag{4}$$

where: k is residence time inside each interconnected reservoir, and n is the number of interconnected reservoirs in the multilinear system. During the present study, the flow stage in Equations (1) and (2) was changed to the concentration. Also, they were rewritten as Equations (5) and (6):

$$C_m = \left(\frac{\Delta t}{\Delta t + k_d}\right)^{n_d} \quad \text{for } m = 1 \tag{5}$$

$$C_m = \left(\frac{k_d}{\Delta t + k_d}\right)\left(\frac{m + n_d - 2}{m - 1}\right) C_{m-1} \quad \text{for } m > 1 \tag{6}$$

where C_1 is the impulse response function of the pollution pulse at $t = \Delta t$, and C_m is the impulse response function of the pollution pulse at $t = m\Delta t$.

During the model operation, each pulse of entrance BC curve was routed using Equations (5) and (6) and the resultant was lagged by $\tau_d/\Delta t$. In which, τ_d is the pure lag of the multilinear model, which can be computed according to

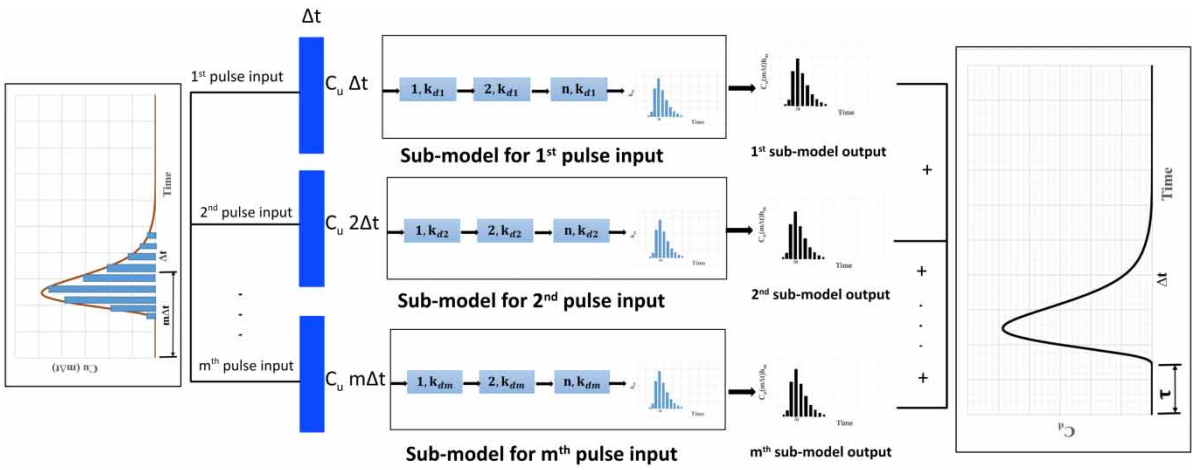

Figure 1 | Framework of multilinear lag cascade (MDLC) simulation procedure.

Equation (7):

$$\tau_d = \tau - \Delta t \tag{7}$$

In the flow routing approaches, it is possible to relate (τ, k, n) parameters to the geometrical and hydraulic characteristics of the river reaches. However, in the pollution transport models, these parameters can be determined using the temporal moments of the BC curve. The nt^h normalized temporal moment (μ_n^*), concerning the time origin, was defined as Equation (8):

$$\mu_n^* = \frac{\mu_n}{\mu_0} = \frac{\int_0^\infty t^n C(x, t)dt}{\int_0^\infty C(x, t)dt} \tag{8}$$

Also, their normalized forms with respect to the mean were defined as Equations (9)–(11) (Schmid 2002):

$$m_1 = \mu_1^* \tag{9}$$

$$m_2 = \mu_2^* - (\mu_1^*)^2 \tag{10}$$

$$m_3 = \mu_3^* - 3\mu_1^*\mu_2^* + 2(\mu_1^*)^3 \tag{11}$$

In which m_{1-3} are normalized temporal moments with respect to the mean of the BC curve. For calculation of the three above-mentioned parameters, the temporal moments from 1st to 3rd order were calculated according to Equations (12)–(14) (Nash 1960):

$$m_1 = nk + \tau \tag{12}$$

$$m_2 = nk^2 \tag{13}$$

$$m_3 = 2nk^3 \tag{14}$$

RESULTS

The MDLC simulation was done with different reach lengths, and an example of the BC curves is shown in Figure 2. As is apparent, it seems from the simulated BC curves that the model performance is desirable, compared to field tracer data. However, since field data were not gathered at regular intervals, theoretical curves cannot accurately match the data intervals. From an observational point of view, it can be said that the model is quite capable of reconstructing concentration-time curves. Notwithstanding this, it was observed that the accuracy of the model decreased with increasing unit length. Furthermore, the model parameters were extracted using central temporal moments (Equations (12)–(14)). It was found that by increasing the reach length and delay time, the number of interconnected reservoirs increased. However, in each of the reservoirs, the resident time of the pollution mass was found to be constant. Moreover, it was observed that increasing the reach flow caused an increase of reservoir residence time (k_d), number of cascading cells (n_d), and delay time (τ_d). The average velocity values (u), calculated from the first-order central moment, showed velocity uniformity is not present in the two studied rivers. As a result, it can be stated that their values were close to each other. However, the longitudinal dispersion coefficients (D) values were increased with increasing units of length, indicating a variable dispersion coefficient at the river reaches. This resulted in an increase in the dispersivity parameter (D/u) in the studied reaches. The skewness coefficient of concentration-time curves also decreased with increasing unit lengths, with its value approximating to 1, thus demonstrating becoming more symmetric in appearance.

As discussed earlier, it is essential to obtain reliable estimations of the modeling length for river reaches. Further research undertaken adopted the classical advection-dispersion equation (ADE) impulse response function as a basic equation (Equation (15)). Then, the synthetic data were generated using it (Ogata & Banks 1961):

$$C(x, t) = \frac{x}{t\sqrt{4\pi Dt}} \exp\left(-\frac{(x - ut)^2}{4Dt}\right) \tag{15}$$

In which A is the cross-sectional area; the distance is x; the average velocity is u, the time is t; and the coefficient of longitudinal dispersion is D.

During the production of synthetic data, a reach with steady uniform velocity of ($u = 20$ m/min) and constant dispersion coefficient $D = 1{,}000$ (m^2/min) was assumed. Fourteen different lengths were selected, assuming constant values of velocity and longitudinal dispersion coefficient, with each representing a particular Pe number. The

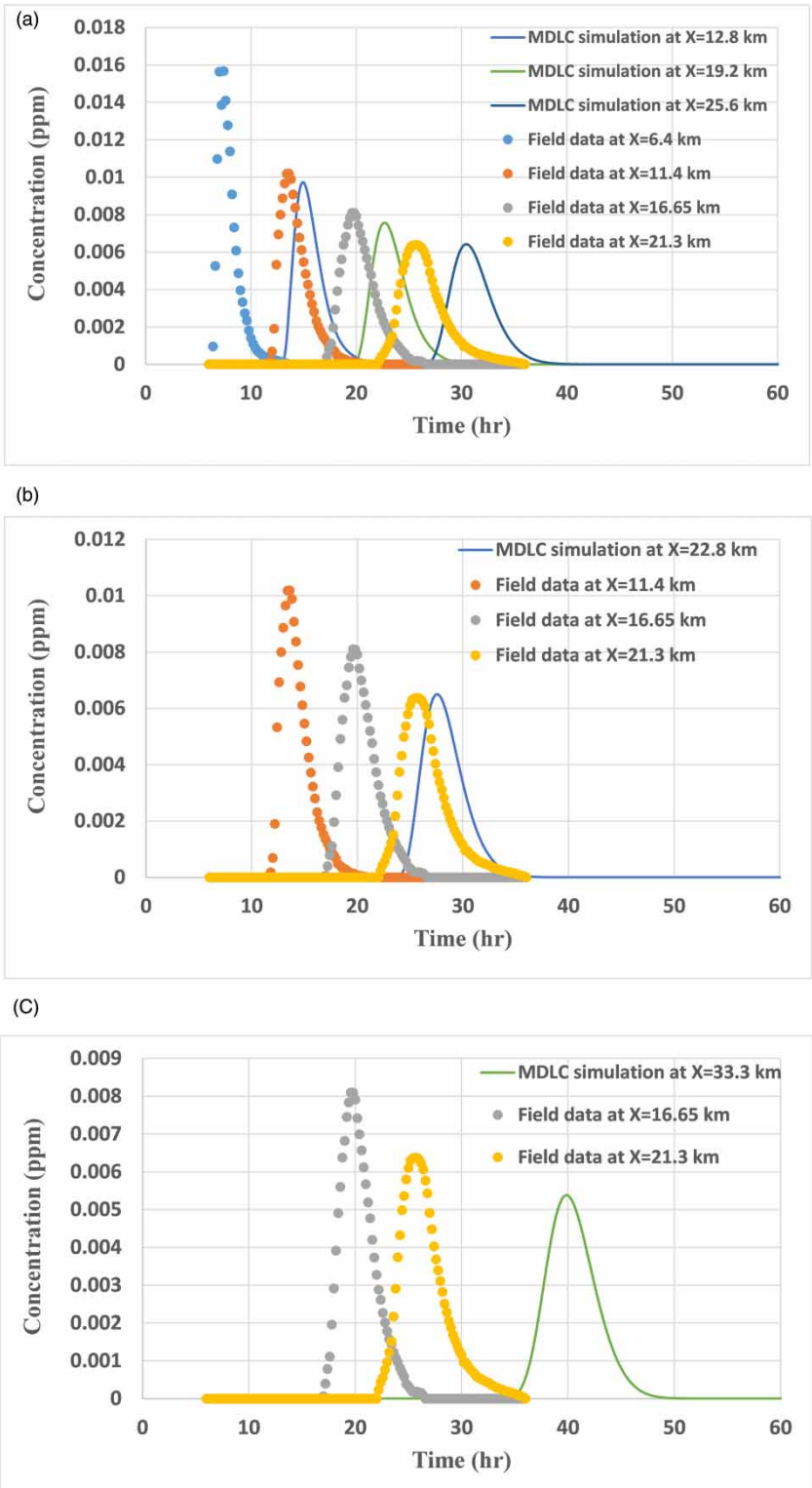

Figure 2 | MDLC simulation versus field data by different reach lengths.

(Pe = (xu/D)) is relating the pollution transportation with average velocity and diffusion process to each other. Selected reach lengths were according to 10, 50, 100, 150, 200, 300, 400, 600, 800, 1,000, 2,000, 5,000, 8,000, and 10,000 m. Therefore, the Peclet numbers calculated from chosen reach values were as follows: 0.1, 1, 2, 3, 4, 6, 8, 12, 16, 20, 40, 100, 160 and 200, respectively. The MDLC model parameters of synthetic BC curves were calculated and plotted against associated Pe numbers; refer to Figure 3.

The plots showed τ_d and n_d parameters increased linearly when the Pe number was increased. Regression lines were established between them and are presented in Figure 3(a) and 3(b). However, k_d was reduced to a constant value of 6.5 hours for all the operated data (Figure 3(c)).

For relating the mean residence times of ADE and MDLC models, four parameters of $(\tau_d)u/\Delta x$, $(\tau_d + k_d)u/\Delta x$, $(n_d \times k_d)u/\Delta x$, $(n_d \times k_d + \tau_d)u/\Delta x$, the synthetic BC curves were calculated and depicted versus Pe numbers (Figure 4). It was found that for values of $Pe \geq 12$, the above-mentioned dimensionless parameters reduce to constant values of 0.33, 0.34, 0.66, 0.98, respectively, which implies that $Pe = 12$ is the base criterion for calculating the unit reach length. Further, $(n_d \times k_d + \tau_d)u/\Delta x$ reduces to 1, which means that the residence time of the pollution in one set of the multilinear group is approximately equal to the ADE model. Hence, it can be concluded that the unit length can be estimated using $\Delta x \approx (12D/u)$. By operating extracted regression equations between Pe number and the number of interconnected reservoirs, the unit length reduced to $x \approx (n_d \times k_d)u/0.66 = 39.76u$. It was obtained at about 795 m for the constant velocity of 20 m/min. It is worth mentioning, however, for regression lines, the length is expressed in the unit of meters and time in minutes. Therefore, the number 39.76 should be multiplied by the average velocity in (m/min) to obtain the interval length in meters.

The reach length for the synthetic data used herein was obtained at about 600 m, 795 m, respectively, using both above-mentioned methods. As discussed earlier, the calculation of MDLC parameters from ADE model parameters would be helpful. Therefore, the theoretical temporal moment relationships were matched between both models to derive the relating equations (Equations (16)–(18)). For the MDLC model, first the reach length has to be estimated, and then its parameters can be determined using

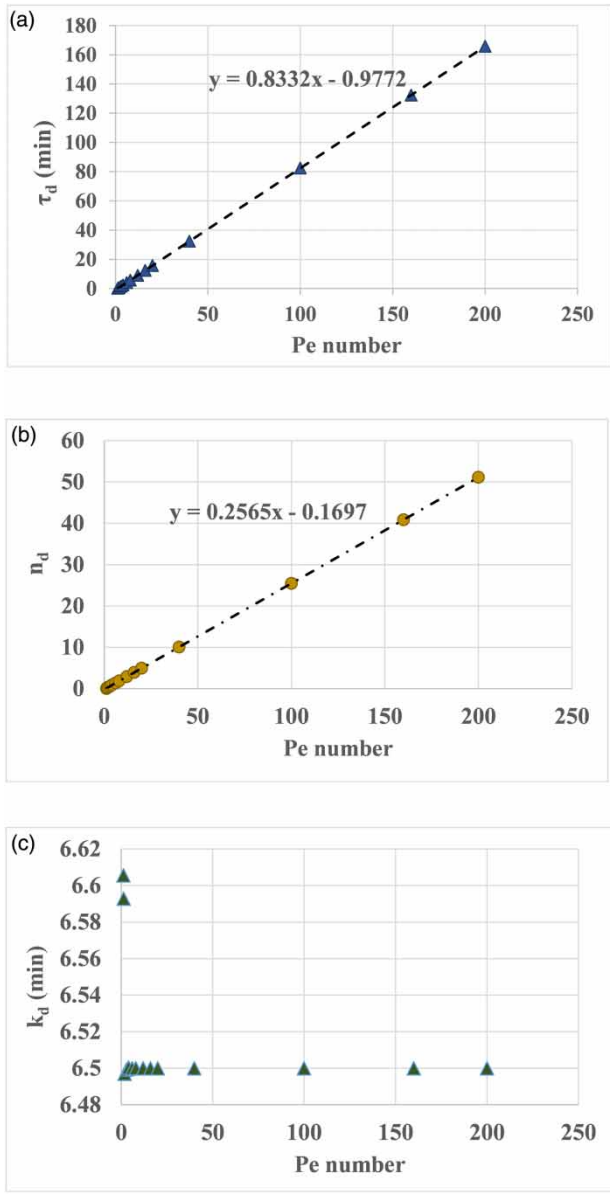

Figure 3 | MDLC parameters associated with synthetic data of ADE unit impulse response function versus Pe number, (a) τ_d versus Pe number, (b) n_d versus Pe number, and (c) k_d versus Pe number.

Equations (16)–(18):

$$k = \frac{D\left(3x^2\sqrt{(u^2/D)} + 16D\sqrt{x^2/x}\right)}{u^2\left(x^2\sqrt{(u^2/D)} + 4D\sqrt{x^2/D}\right)} \tag{16}$$

$$n = \frac{2\left(x^2\sqrt{(u^2/D)} + 4D\sqrt{x^2/D}\right)^3}{D\sqrt{x^2/D}\left(3x^2\sqrt{(u^2/D)} + 16D\sqrt{x^2/D}\right)^2} \tag{17}$$

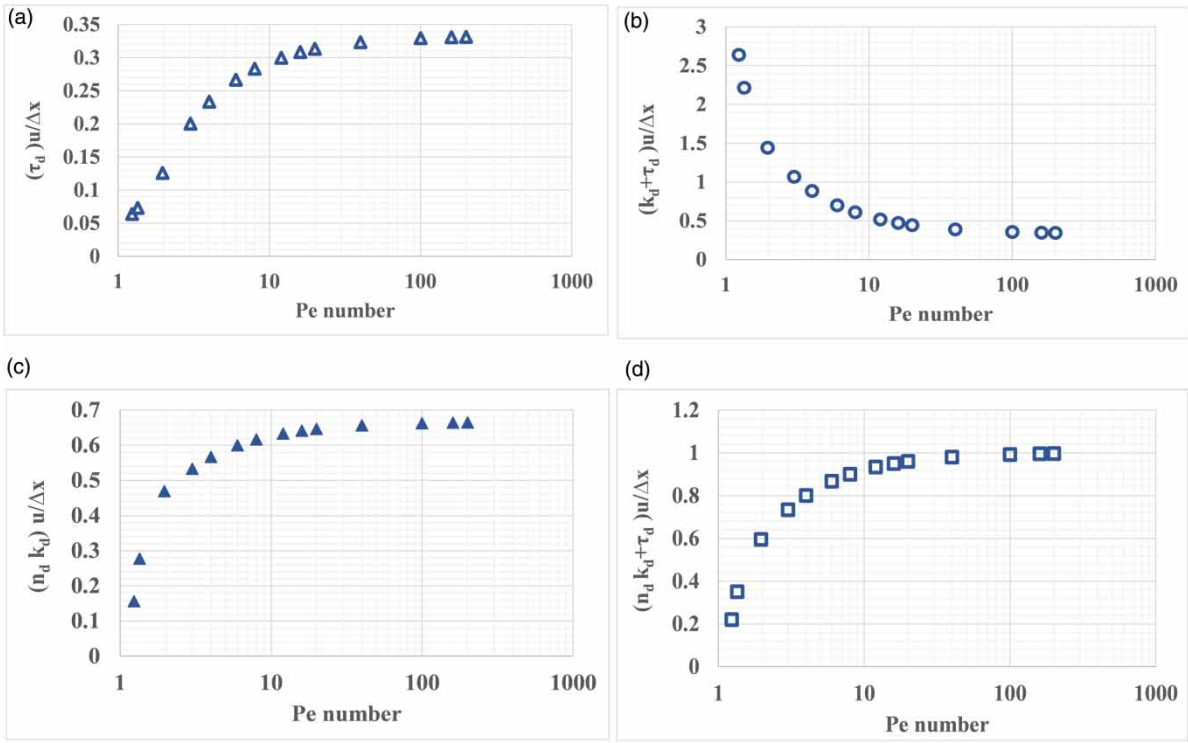

Figure 4 | (a) Variation of $(\tau_d)u/\Delta x$ versus Pe number, (b) variation of $(\tau_d + k_d)u/\Delta x$ versus Pe number, (c) variation of $(n_d \times k_d)u/\Delta x$ versus Pe number, (d) variation of $(n_d \times k_d + \tau_d)u/\Delta x$ versus Pe number.

$$\tau = \frac{x^2\left(6D^2\sqrt{u^2/D}\sqrt{(x^2/D)} + x^2u^2\right)}{u^2D\sqrt{x^2/D}\left(3x^2\sqrt{(u^2/D)} + 16D\sqrt{x^2/D}\right)} \quad (18)$$

Ghosh *et al.* (2008) tried to relate the hybrid cells in series parameters to the average flow velocity by fixing the dispersivity parameter (D/u) to a constant value and extracting the proportionality coefficient. The same procedure was operated to examine MDLC model parameters for different combinations of u and D. For this purpose, four different combinations of average velocity and dispersion coefficient were selected, with all having equal ratios. Then, the ratios of (n_{d2}/n_{d1}), (τ_{d2}/τ_{d1}), (k_{d2}/k_{d1}) were examined using u_2/u_1 and the results are depicted in Figure 5.

It can be concluded that, like the hybrid cellular model, the MDLC parameters changed concerning the ratio of velocities. It is shown in Figure 5(a) that by increasing the average velocity through the river reach, the number of cascading reservoirs increased. However, no explicit and general relationship can be deduced from this curve. Therefore, a relationship has to be established in the first instance between (n_d) and Pe number followed by another equation being derived between velocity and the proportionality coefficient. Finally, combining both equations resulted in Equation (19).

Moreover, the delay time (τ_d) variation was studied with increasing average velocity, and it was concluded that by increasing flow velocity, the delay time reduced. The regression equations, specified in Figure 5(b), showed that there is a reverse relationship between them. In other words, for example, by quadrupling the flow velocity, the delay time would become one quarter (Equation (20)). From Equation (20), the regression equations between residence time and flow velocity were extracted. An inverse correlation was found with changes exhibiting an exponential pattern (Figure 5(c)). The extracted relationship was also given as Equation (21):

$$\frac{n_{d2}}{n_{d1}} = \frac{(0.0035\,u_2 + 0.1765)}{(0.0035\,u_1 + 0.1765)} \times \left(\frac{u_2}{u_1}\right)\left(\frac{D_1}{D_2}\right) \quad (19)$$

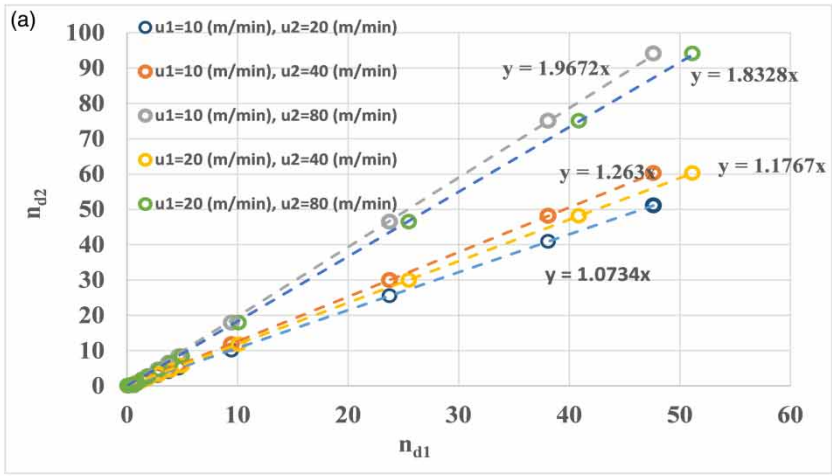

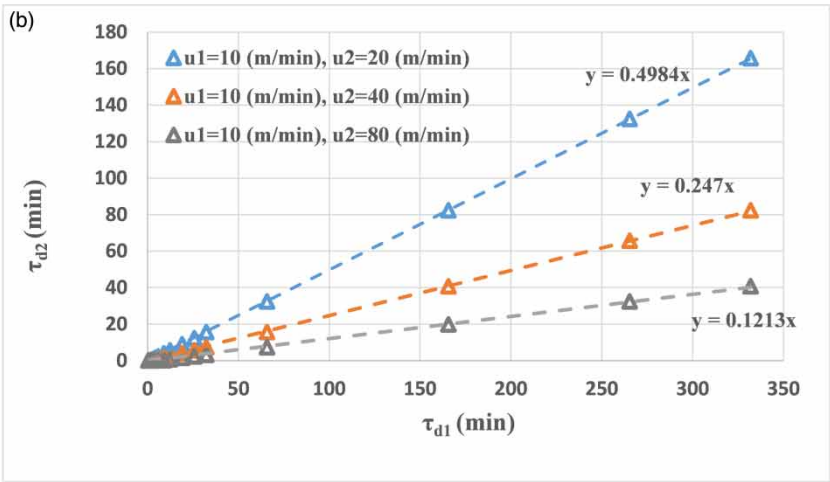

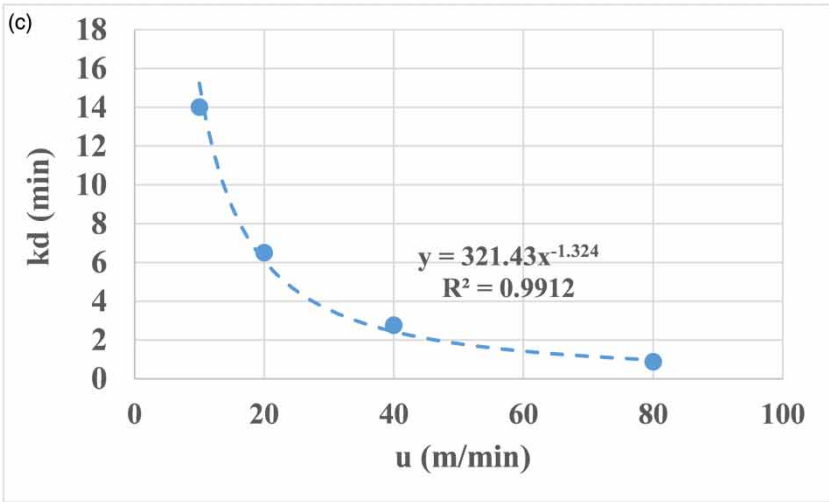

Figure 5 | (a) Relationship between the numbers of reservoirs (n_d) at different velocities, (b) relationship between delay times (τ_d) at different velocities, (c) relationship between average flow velocity and cell residence time (k_d).

$$\frac{\tau_{d2}}{\tau_{d1}} = \left(\frac{u_1}{u_2}\right) \tag{20}$$

$$\frac{k_{d2}}{k_{d1}} = \left(\frac{u_1}{u_2}\right)^{1.324} \tag{21}$$

Sensitivity analysis

In this section, firstly, the sensitivity of MDLC model parameters to the dispersion coefficient (D), average flow velocity (u), and interval length (x) was examined. In each step, the parameter changed over a selected range assuming two other parameters were kept constant. Then, the increasing or decreasing trend of the MDLC parameters and their variation slope were investigated. Equation (22) was used to make the numerical ranges of length, velocity and dispersion coefficient uniform:

$$y_n = \frac{(y_i - \bar{y})}{\text{std}(y)} \tag{22}$$

where y_n is the normalized parameter, $\bar{y}$ is the mean of the (y) parameter, and std(y) is the standard deviation of the (y) parameter. The selected ranges of ADE parameters were chosen from Equation (23). Also, the results of sensitivity analysis versus parameter variations are shown in Figure 6:

$$0 \le x \le 10000\ (\text{m}),\ 0 \le u \le 3\left(\frac{\text{m}}{\text{s}}\right),\ 0 \le D \le 0.5\left(\frac{\text{m}^2}{\text{s}}\right) \tag{23}$$

It was determined that velocity, dispersion coefficient and length parameters have the most to least effects on the estimation of residence time, respectively (Figure 6(a)). Furthermore, variation of reach length does not affect the value of residence time. In terms of velocity and dispersion coefficient parameters, they have a decreasing and increasing influence on the residence time, respectively. Also, a decreasing trend of velocity was found to be in exponential form, whilst an increasing trend of dispersion coefficient was found to be linear. It was also revealed that velocity and

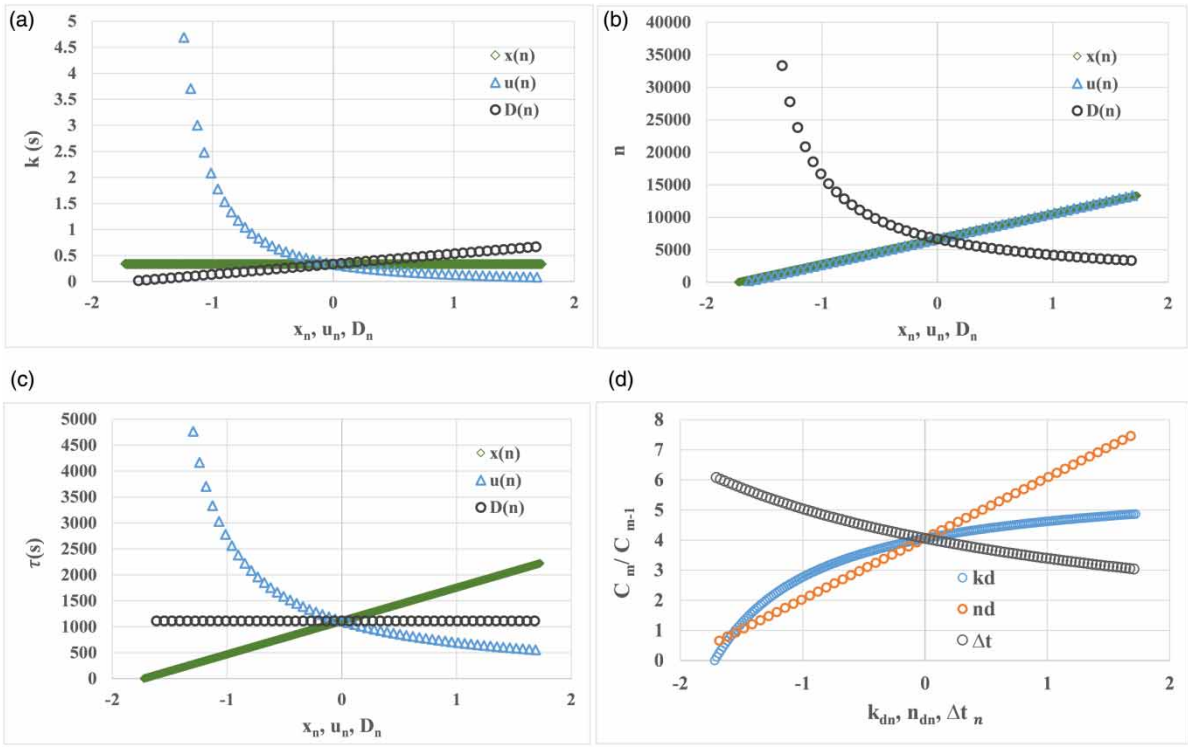

Figure 6 | (a) Sensitivity of parameter (k) to length, velocity and dispersion coefficient variations, (b) sensitivity of parameter (n) to length, velocity and dispersion coefficient variations, (c) sensitivity of parameter (τ) to length, velocity and dispersion coefficient variations, and (d) sensitivity of (C_m/C_{m-1}) to variation of k_d, n_d, and τ_d.

distance parameters give the same linear incremental effect on the number of cascading cells, as seen in Figure 6(b). However, increasing the coefficient of longitudinal dispersion caused the number of cascading cells to decrease nonlinearly.

Consequently, the change in the longitudinal dispersion coefficient was found to have no effect on the delay time. However, velocity and reach length have decreasing and incremental effects on delay time estimation, respectively (Figure 6(c)). In conclusion, the parameters of velocity, dispersion coefficient and velocity have the most influence on the estimation of residence time, cascade cell number and delay time, respectively. Additionally, the sensitivity of Equation (6) to the three constituent parameters was investigated, and the results are shown in Figure 6(d). In this figure, the non-dimensional parameter of C_m/C_{m-1} is shown versus k_d, n_d, and Δt, respectively. As for the number of cascade cells (n_d), this was found to have the most significant effect on the concentration values rather than the other two parameters. Also, by increasing the discretized time (Δt), it reduced the dimensionless concentration in two consecutive time steps. From this, it appears that increasing the residence time (k_d) of the contaminants inside the cascade cells by certain amounts will have no specific effect on the concentration value.

CONCLUSION

The operation of pollutant transport models that are simple and accurate enough is preferred for environmental issues. Multilinear models can generate dynamic properties of contaminant pollution graphs. Because of the similarity of flow hydrographs and contaminant concentration curves, the multilinear lag cascade (MDLC) model was selected for performance testing. The results showed the efficacy of the mentioned model in contaminant transport simulation, but issues regarding its operation have to be considered. It was found that the length unit should be estimated using $\Delta x \approx (12D/u)$, which was found by correlating MDLC with the conventional classical Advection Dispersion Equation (ADE). Additionally, by operation of the derived equations, the unit length was reduced to $x \approx (n_d \times k_d)u/0.66 = 39.76u$. Moreover, it was found that by increase in the Peclet number the non-dimensional parameter of $(n_d \times k_d + \tau_d)u/\Delta x$ is reduced to 1, which indicates that the residence time of the contaminant mass through the unit length is equal to the passage time of pollution in the ADE model. A comparison between hybrid cells in series and MDLC models indicated that their parameters varied by changes in the average flow velocity. By an increase in flow velocity, the number of cascades is increased and, conversely, both the resident and delay time parameters were decreased. The sensitivity analysis was performed to consider the importance of MDLC parameters in BC curve simulation. The study concluded that the number of cascading reservoirs is the most significant parameter in the creation of theoretical BC curves.

CONFLICT OF INTEREST

None.

DATA AVAILABILITY STATEMENT

All relevant data are included in the paper or its Supplementary Information.

REFERENCES

Azamathulla, H. M. & Ahmad, Z. 2012 Gene-expression programming for transverse mixing coefficient. *Journal of Hydrology* **434–435C**, 142–148.

Azamathulla, H. M. & Wu, F.-C. 2011 Support vector machine approach for longitudinal dispersion coefficients in streams. *Applied Soft Computing* **11** (2), 2902–2905.

Battiato, I. & Rubol, S. 2014 Single-parameter model of vegetated aquatic flows. *Water Resources Research* **50**, 6358–6369.

Bhabagrahi, S., Perumal, M., Moramarco, T., Barbetta, S. & Sahoo, S. 2019 A multilinear discrete Nash-cascade model for stage-hydrograph routing in compound river channels. *Hydrological Sciences Journal*. doi:10.1080/02626667.2019.1699243.

Becker, A. 1976 Simulation of nonlinear flow systems by combining linear models. In: *Moscow Symposium, 1971, Mathematical Models in Geophysics*, Wallingford, UK. International Association of Hydrological Sciences, IAHS Publ. 116, pp. 135–142.

Becker, A. & Kundzewicz, Z. W. 1987 Nonlinear flood routing with multilinear models. *Water Resources Research* **23** (6), 1043–1048.

Bencala, K. E. & Walters, R. A. 1983 Simulation of solute transport in a mountain pool and riffle stream: a transient storage model. *Water Resources Research* **19** (3), 718–724.

Boano, F., Packman, A. I., Cortis, A., Revelli, R. & Ridolfi, L. 2007 A continuous time random walk approach to the stream transport of solutes. *Water Resources Research* **43**, W10425.

Boano, F., Harvey, J. W., Marion, A., Packman, A. I., Revelli, R., Ridolfi, L. & Worman, A. 2014 Hyporheic flow and transport processes: mechanisms, models, and biogeochemical implications. *Reviews of Geophysics* **52**, 603–679.

Bottacin-Busolin, A., Marion, A., Musner, T., Tregnaghi, M. & Zaramella, M. 2011 Evidence of distinct contaminant transport patterns in rivers using tracer tests and a multiple domain retention model. *Advances in Water Resources* **34** (6), 737–746.

Breugem, W. P., Boersma, B. J. & Uittenbogaard, R. E. 2006 The influence of wall permeability on turbulent channel flow. *Journal of Fluid Mechanics* **562**, 35–72.

Briggs, M. A., Gooseff, M. N., Arp, C. D. & Baker, M. A. 2009 A method for estimating surface transient storage parameters for streams with concurrent hyporheic storage. *Water Resources Research* **45** (4), W00D27.

Camacho, L. A. & Lees, M. J. 1999 Multilinear discrete lag-cascade model for channel routing. *Journal of Hydrology* **226** (1), 30–47.

Chabokpour, J. 2020 Study of pollution transport through the rivers using aggregated dead zone and hybrid cells in series models. *International Journal of Environmental Science and Technology*. https://doi.org/10.1007/s13762-020-02741-w.

Chandler, I. D., Guymer, I., Pearson, J. M. & van Egmond, R. 2016 Vertical variation of mixing within porous sediment beds below turbulent flows. *Water Resources Research* **52** (5), 3493–3509.

Choi, J., Harvey, J. W. & Conklin, M. H. 2000 Characterizing multiple timescales of stream and storage zone interaction that affect solute fate and transport in streams. *Water Resources Research* **36** (6), 1511–1518.

Cimorelli, L., Cozzolino, L., D'Aniello, A. & Pianese, D. 2018 Exact solution of the Linear Parabolic Approximation for flow-depth based diffusive flow routing. *Journal of Hydrology* **563**, 620–632.

de Lemos, M. J. S. 2005 Turbulent kinetic energy distribution across the interface between a porous medium and a clear region. *International Communications in Heat and Mass Transfer* **32** (1–2), 107–115.

Deng, Z., Bengtsson, L. & Singh, V. P. 2006 Parameter estimation for fractional dispersion model for rivers. *Environmental Fluid Mechanics* **6** (5), 451–475.

Elder, J. W. 1959 The dispersion of marked fluid in turbulent shear flow. *Journal of Fluid Mechanics* **5** (04), 544–560.

Fischer, H. B. 1966 *Longitudinal Dispersion in Laboratory and Natural Streams*, Tech. Rep. KH-R-12. Calif. Inst. of Technol., Pasadena.

Fischer, H. B. 1967 The mechanics of dispersion in natural streams. *Journal of Hydraulic Engineering* **93** (6), 187–216.

Fischer, H. B. 1968 Dispersion predictions in natural streams. *Journal of the Sanitary Engineering Division* **94** (5), 927–944.

Ghosh, N. C., Mishra, G. C. & Kumarasamy, M. 2008 Hybrid-cells-in-series model for solute transport in streams and relation of its parameters with bulk flow characteristics. *Journal of Hydraulic Engineering* **134**, 497–502.

Godfrey, R. G. & Frederick, B. J. 1963 *Dispersion in Natural Streams*, USGS Unnumbered Ser. U.S. Geol. Surv., Washington, DC.

Gooseff, M. N., McKnight, D. M., Runkel, R. L. & Duff, J. H. 2004 Denitrification and hydrologic transient storage in a glacial meltwater stream, McMurdo Dry Valleys, Antarctica. *Limnology and Oceanography* **49** (5), 1884–1895.

Gooseff, M. N., Briggs, M. A., Bencala, K. E., McGlynn, B. L. & Scott, D. T. 2013 Do transient storage parameters directly scale in longer, combined stream reaches? Reach length dependence of transient storage interpretations. *Journal of Hydrology* **483**, 16–25.

Haggerty, R., McKenna, S. A. & Meigs, L. C. 2000 On the late-time behavior of tracer test breakthrough curves. *Water Resources Research* **36** (12), 3467–3479.

Hays, J. R., Krenkel, P. A. & Schnelle, K. B. 1966 *Mass Transport Mechanisms in Open-Channel Flow, Technical report No. 8*. Dept. of Civ. Eng., Vanderbilt Univ., Nashville, TN, p. 138.

Higashino, M., Clark, J. J. & Stefan, H. G. 2009 Pore water flow due to near-bed turbulence and associated solute transfer in a stream or lake sediment bed. *Water Resources Research* **45** (12). doi:10.1029/2008WR007374.

Jackson, T. R., Haggerty, R. & Apte, S. V. 2013 A fluid-mechanics based classification scheme for surface transient storage in riverine environments: quantitatively separating surface from hyporheic transient storage. *Hydrology and Earth System Sciences* **17** (7), 2747–2779.

Keefer, T. N. & McQuivey, R. S. 1974 Multiple linearization flow routing model. *Journal of Hydraulic Division* **100** (HY7), 1031–1046.

Kelly, J. F., Bolster, D., Meerschaert, M. M., Drummond, J. D. & Packman, A. I. 2017 Fracfit: a robust parameter estimation tool for fractional calculus models. *Water Resources Research* **53** (3), 2559–2567.

Kundzewicz, Z. W. 1984 Multilinear flood routing. *Acta Geophysica, Pol.* **32** (4), 419–445.

Marion, A., Zaramella, M. & Bottacin-Busolin, A. 2008 Solute transport in rivers with multiple storage zones: the STIR model. *Water Resources Research* **44**, W10406.

Musner, T., Bottacin-Busolin, A., Zaramella, M. & Marion, A. 2014 A contaminant transport model for wetlands accounting for distinct residence time bimodality. *Journal of Hydrology* **515**, 237–246.

Nash, J. E. 1960 , a unit hydrograph study with particular reference to British catchments. *Proceedings of the Institution of Civil Engineers* **17**, 249–282.

Nepf, H. M. 2012 Flow and transport in regions with aquatic vegetation. *Annual Review of Fluid Mechanics* **44** (1), 123–142.

Nordin, C. F. & Sabol, G. V. 1974 Empirical data on longitudinal dispersion in rivers. *Water-Resources Investigations* 20–74. U.S. Geological Survey, Denver, CO.

O'Connor, K. M. 1976 A discrete linear cascade model for hydrology. *Journal of Hydrology* **29** (3–4), 203–242.

Ogata, A. & Banks, R. B. 1961 *A Solution of the Deferential Equation of Longitudinal Dispersion in Porous Media*, Professional Paper No. 411-A. U.S. Geological Survey, Denver, CO.

Pedersen, F. B. 1977 *Prediction of Longitudinal Dispersion in Natural Streams*, Tech. Rep. Ser. Pap. 14. Inst. of Hydrodyn. and Hydraul. Eng., Tech. Univ. of Denmark, Lyngby.

Perumal, M. 1992 Multilinear Muskingum flood routing method. *Journal of Hydrology* **133** (34), 259–272.

Perumal, M. 1994 Multilinear discrete cascade model for channel routing. *Journal of Hydrology* **158** (1–2), 135–150.

Perumal, M. & Sahoo, B. 2007 Applicability criteria of the variable parameter Muskingum stage and discharge routing methods. *Water Resources Research* **43** (5), 1–20, W05409.

Roche, K. R., Li, A., Bolster, D., Wagner, G. J. & Packman, A. I. 2019 Effects of turbulent hyporheic mixing on reach-scale transport. *Water Resources Research*. doi:10.1029/2018WR023421.

Rubol, S., Battiato, I. & de Barros, F. P. J. 2016 Vertical dispersion in vegetated shear flows. *Water Resources Research* **52**, 8066–8080.

Sayre, W. W. & Chang, F. M. 1968 *A Laboratory Investigation of Open-Channel Dispersion Processes for Dissolved, Suspended, and Floating Dispersants*, USGS Professional Paper, 433-E. US Government Printing Office, Washington.

Schmid, B. 2002 Persistence of skewness in longitudinal dispersion data: can the dead zone model explain it after all? *Journal of Hydraulic Engineering* **128** (9), 848–854.

Sherman, T., Roche, K. R., Richter, D. H., Packman, A. I. & Bolster, D. 2019 A Dual Domain stochastic Lagrangian model for predicting transport in open channels with hyporheic exchange. *Advances in Water Resources* **125**, 57–67.

Shucksmith, J. D., Boxall, J. B. & Guymer, I. 2010 Effects of emergent and submerged natural vegetation on longitudinal mixing in open channel flow. *Water Resources Research* **46**, W04504.

Spada, E., Sinagra, M., Tucciarelli, T., Barbetta, S., Moramarco, T. & Corato, G. 2017 Assessment of river flow with significant lateral inflow through reverse routing modeling. *Hydrological Processes* **31**, 1539–1557.

Taylor, G. 1953 Dispersion of soluble matter in solvent flowing slowly through a tube. *Proceedings of the Royal Society of London. Series A. Mathematical and Physical Sciences* **219** (1137), 186–203. doi:10.1098/rspa.1953.0139.

Taylor, G. 1954 The dispersion of matter in turbulent flow through a pipe. *Proceedings of the Royal Society of London. Series A. Mathematical and Physical Sciences* **223** (1155), 446–468. doi:10.1098/rspa.1954.0130.

Voermans, J. J., Ghisalberti, M. & Ivey, G. N. 2017 The variation of flow and turbulence across the sediment–water interface. *Journal of Fluid Mechanics* **824**, 413–437. doi:10.1017/jfm.2017.345.

First received 30 May 2020; accepted in revised form 24 July 2020. Available online 10 August 2020